Mixed signatures for subcritical dynamics in rodent hippocampus during sleep and awake epochs

Pranjal Garg[a]

Neuronal dynamics such as brain criticality have recently been attributed to optimal information processing. Brain criticality attempts to elucidate the collective dynamics of a large number of neurons. It posits that the brain operates near critical to the critical point, although the field is rife with controversies and contrasting evidence. Similar computational capacities are observed during sharp wave ripples in the hippocampus prompting the need to correlate their dynamics. In the current study, we report the measures of avalanche criticality including neuronal avalanches, branching process, crackling noise relation, and deviation from criticality coefficient and Hurst exponents for long-range temporal correlations in rodent hippocampus during sharp wave ripples. We found evidence for mixed subcritical to critical dynamics in the hippocampus and minimal difference between ripple and no ripple times across measured metrics. The evidence demonstrates heterogeneity in signatures of criticality among animals and brain areas, indicating the presence of broad-range neuronal dynamics.

Criticality | Sharp wave ripples | Hippocampus

Criticality, as borrowed from statistical physics has gained traction in recent years to elucidate the complex dynamics of the brain. It marks the transition between disordered state (subcritical) to asynchronous ordered state (supercriticality) (1). This is poised to enable the neural system to respond effectively to external stimuli, transmit information efficiently, optimally compute and store memories effectively (1, 2). Evidence of criticality or near-criticality phenomenon has been observed in several brain regions including the hippocampus and in both awake and sleep epochs (3–5). In the hippocampus sharp wave ripples Fig 1. (a) during both sleep and awake periods have also been observed. These unique neural activities are believed to play a role in memory retrieval and consolidation and planning (6). The bulk of sharp wave ripples (SWRs) are marked by memory replay, the spontaneous reactivation of neural patterns similar to those seen during past waking experiences (7). They are also a candidate for bidirectional information flow between hippocampus and cortex (8). The intersection of these functions motivated us to explore the criticality in the hippocampus during ripples.

Determination of avalanche criticality requires multiple estimation strategies. To do this, we accessed a previously published dataset of hippocampal local field potential (LFP) recordings in 10 rodents (7, 9). The avalanches, their size and duration, were obtained by dividing the LFP into two sets- ripple times and no ripple times. Then we clustered the avalanches for each animal and each epoch before estimating the avalanche metrics.

Results

Traditionally, criticality has been experimentally determined by the presence of neuronal avalanches, the spontaneous cascades of neural activity (Fig. 1 (b)) characterized by power-law distributions in terms of their size and duration (10).

$$P(S) \sim S^{-\alpha}$$
$$P(T) \sim S^{-\tau}$$

We identified neuronal avalanches in four epochs and computed the power law exponents α and τ (Fig 1. (c)). To discretize and identify the suprathreshold events in local field potential signals (LFP) we applied variable standard deviations (SD) and bin sizes. We found near constant power law exponents before the cut-off marked by the size of avalanches

Author affiliations: [a]All India Institute of Medical Sciences, Rishikesh, Virbhadra Road, Rishikesh · Uttarakhand- 249203, India

The authors have no competing interests to declare

[1]To whom correspondence should be addressed. E-mail: pranjaldungmail.com

obeying power law. The power law was preserved for varying SD for both avalanche size and lifetime, with nearly equivalent power law exponents indicating threshold scale invariance and thus describing fractal avalanche organization. Similarly, it was preserved for different bin sizes and as expected the absolute value of the exponent increased with increasing bin size, an empirical demonstration of temporal scale-invariance. To estimate the fit of the power law for the size of the avalanches we generated synthetic power law data, compared Kolmogorov Smirnov statistic with empirical distribution, and defined p-values as the deviation from power law by empirical data compared to each synthetic data (n = 1000). We found that size and avalanches had statistically significant power law distribution. These findings are consistent with criticality in the brain during both ripples and no ripples throughout sleep and awake epochs. However, the duration distribution followed power law for only one order of magnitude before cutting off.

Original studies showed power law exponents for the size of $\alpha \sim 3/2$ and for the duration of $\tau \sim 2$. In contrast, we found variable values of power law exponents, although τ values were generally higher than α values (Fig 1. (d) and Fig. 1 (e)). For different epochs, awake during no ripples ($\alpha = 1.79 \pm 0.14$), awake during ripples ($\alpha = 1.75 \pm 0.11$), sleep during no ripples ($\alpha = 1.79 \pm 0.13$) and sleep during ripples ($\alpha = 1.77 \pm 0.11$) we found significant differences in the α values during awake and sleep epochs and during ripples and no ripples during awake epoch (Fig. 1 (f)). The findings of actual values of power law exponents are however controversial and do not indicate either the absence or presence of criticality.

To evaluate criticality more rigorously, we assessed crackling noise scaling relations. Scaling theory predicts the distribution between mean sizes conditioned on a specific duration.

$$< S > (T) \sim T^{\frac{1}{\sigma v Z}}$$

Here, σ, v, and z are other critical exponents of the system (σ is not the branching parameter). In Fig. 1 (g) we have demonstrated the linear fit to determine the exponent $\lambda_{fit} = \frac{1}{\sigma v z}$, for the distribution of an epoch. At the critical point, the scaling theory satisfies the relation,

$$\frac{\tau - 1}{\alpha - 1} = \frac{1}{\sigma v z}$$

In the current paper, we found that none of the epochs satisfied the scaling relation as shown in Fig. 1 (h), ($\lambda_{predict} = (\tau - 1)/(\alpha - 1)$) indicating possible deviation from criticality. To quantify this distance from criticality we computed Deviation from Criticality coefficient defined as (11),

$$DCC = |\lambda_{predict} - \lambda_{fit}|$$

We found a significant difference in DCC (Fig. 1 (i)) between sleep and awake epochs during both ripple and no ripple times, wherein sleep no ripples showed the maximum proximity to criticality. Furthermore, we found variable DCC in different animals. Some animals showed critical dynamics ($DCC < 0.2$) indicating interindividual differences (Fig. 1 (j)). To classify the system further into supercritical, subcritical, and critical states we estimated the branching parameter given by

$$\sigma = \frac{1}{N} \sum_{j=1}^{N} \frac{n_{events} \text{ in second bin of } j^{th} \text{ avalanche}}{n_{events} \text{ in first bin of } j^{th} \text{ avalanche}}$$

where N is the total avalanches in the specific epoch and n_{events} is the total suprathreshold events in the specific bin. In Fig. 1 (k) we found that in all epochs the system was primarily subcritical ($\sigma < 0.5$). Fig. 1 (l) demonstrates the phase plot of the branching parameter vs avalanche size exponent relationship, with mean values far from $\sigma = 1$ and $\alpha = 1.5$ suggesting subcriticality in the system. Except for one animal (*remy* in Fig. 1 (e), Fig. 1 (f) and Fig. 1 (m)), all other animals followed this trend. To quantify the differences between individual animals, we calculated the mean Wasserstein distance, weighted by counts, for the distributions of avalanche size and duration. In Fig. 1 (n), *remy* showed the maximum distance from the rest of the animals ($W = 7.3 \pm 2.68$). Although the animals *bon*, *fra*, and *dud* showed critical dynamics in Fig. 1 (j), they did not have avalanche profiles different from other animals and could indicate natural variability or undesirable and unobserved experimental noise.

Next, we quantified the long-range temporal correlations (LRTC) which are considered one of the cardinal signs of criticality. We applied unbiased detrended fluctuation analysis (UDFA) to estimate the scaling exponent or Hurst exponent (H) (12). The value H in the range of 0.5-1 indicates a time series with non-trivial long-term positive autocorrelation, signifying the presence of LRTC. In Fig. 2 we explored Hurst exponents for four epochs for delta band (<4 Hz), theta band (4–8 Hz), alpha band (8–12 Hz), beta band (12–30 Hz), and gamma bands (30–80 Hz). As expected, exponents were generally larger during sleep than during awake (13). We found the largest exponents for 55-80 Hz (in the gamma band) across all epochs closely followed by exponents in 21-30 Hz (in the beta band). We hypothesize that the observed LRTC might influence the initiation and propagation of SWRs, emphasizing some role of criticality in shaping ripples.

Overall, we discovered mixed signatures of subcriticality in the hippocampus in contrast to previous evidence in calcium imaging studies (3). Subcriticality is marked by focussed attention, response specificity to stimulus, and stimulus detection among others as compared to supercriticality (2). The dominance of subcriticality over supercriticality is also said to control brain activity from becoming epileptic. The mixed signatures and variability in different individuals and previous attempts could possibly be reconciled by the presence of heterogeneous neuronal dynamics across regions (14). It has been suggested that the hippocampus operates closer to criticality when performing cognitive tasks. However, in the current study, we analyzed criticality during sleep and awake (run) epochs, uncovering the likelihood of subcritical to near critical dynamics during tasks requiring less cognitive capacity (3) in contrast to cortical structures (15). Heterogeneity in results could also be due to experimental and estimation methodology-induced variability. We further found a non-significant difference between ripples and no ripple times, validating the possibility that criticality itself might be limited in optimizing information processing seen specifically during ripples in the hippocampus.

1. Y Tian, et al., Theoretical foundations of studying criticality in the brain. *Netw. Neurosci.* **6**, 1148–1185 (2022).
2. J O'Byrne, K Jerbi, How critical is brain criticality? *Trends Neurosci.* (2022).
3. F Habibollahi, D Sun, AN Burkitt, C French, Neural networks are tuned near criticality during a cognitive task and distanced from criticality in a psychopharmacological model of alzheimer's disease. *bioRxiv* pp. 2023–08 (2023).
4. B Mariani, et al., Neuronal avalanches across the rat somatosensory barrel cortex and the effect of single whisker stimulation. *Front. systems neuroscience* **15**, 709677 (2021).
5. V Priesemann, M Valderrama, M Wibral, M Le Van Quyen, Neuronal avalanches differ from wakefulness to deep sleep–evidence from intracranial depth recordings in humans. *PLoS computational biology* **9**, e1002985 (2013).
6. W Tang, SP Jadhav, Sharp-wave ripples as a signature of hippocampal-prefrontal reactivation for memory during sleep and waking states. *Neurobiol. learning memory* **160**, 11–20 (2019).
7. EL Denovellis, et al., Hippocampal replay of experience at real-world speeds. *Elife* **10**, e64505 (2021).
8. R Pedrosa, et al., Hippocampal gamma and sharp wave/ripples mediate bidirectional interactions with cortical networks during sleep. *Proc. Natl. Acad. Sci.* **119**, e2204959119 (2022).
9. E Denovellis, et al., Data from: Hippocampal replay of experience at real-world speeds (2021).
10. JM Beggs, D Plenz, Neuronal avalanches in neocortical circuits. *J. neuroscience* **23**, 11167–11177 (2003).
11. Z Ma, GG Turrigiano, R Wessel, KB Hengen, Cortical circuit dynamics are homeostatically tuned to criticality in vivo. *Neuron* **104**, 655–664 (2019).
12. Q Yuan, C Gu, T Weng, H Yang, Unbiased detrended fluctuation analysis: Long-range correlations in very short time series. *Phys. A: Stat. Mech. its Appl.* **505**, 179–189 (2018).
13. C Meisel, K Bailey, P Achermann, D Plenz, Decline of long-range temporal correlations in the human brain during sustained wakefulness. *Sci. reports* **7**, 11825 (2017).
14. LL Gollo, Coexistence of critical sensitivity and subcritical specificity can yield optimal population coding. *J. The Royal Soc. Interface* **14**, 20170207 (2017).
15. ED Fagerholm, et al., Cascades and cognitive state: focused attention incurs subcritical dynamics. *J. Neurosci.* **35**, 4626–4634 (2015).

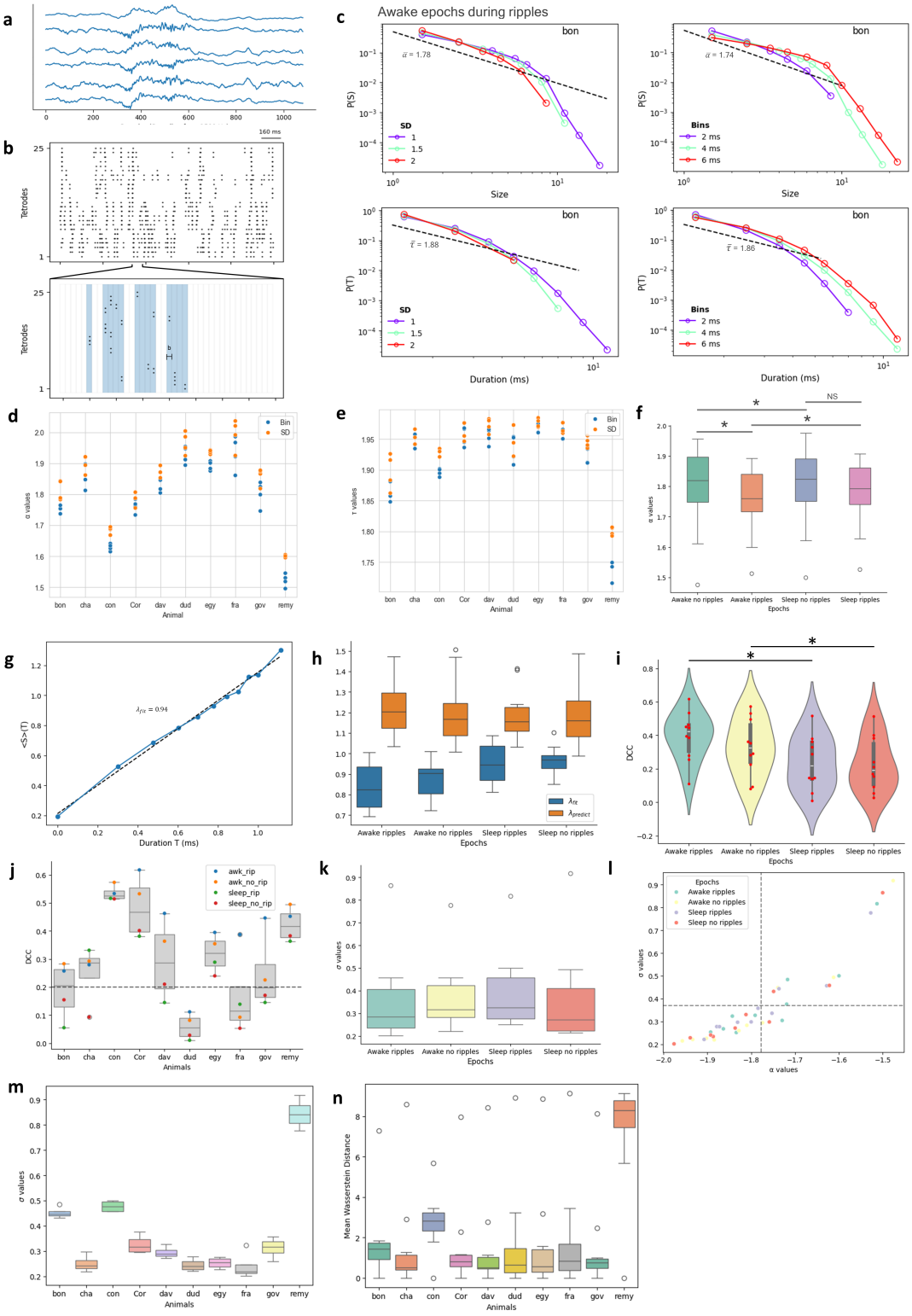

Figure 1. Avalanche metrics and branching metrics of avalanche criticality.

(a) Plot of local field potential (LFP) with sharp wave ripples characterized by high synchronous neural activity. **(b)** Raster plot of suprathreshold activity extracted from LFP and clustered (blue) with bin size b to define avalanche distribution. Each avalanche is bound by bins of no activity. **(c)** Power law distribution of avalanches for variable thresholds (left panel) and bin sizes (right panels) before cutting off after a few orders of magnitudes (for size) and a single order of magnitude (for duration). Upper panels represent avalanche size and lower panels represent avalanche durations. Each figure is plotted as a representation of a single epoch in one animal. **(d)** Avalanche size exponents (α) and **(e)** duration exponents (τ) for variable threshold and bin sizes are plotted against all animals. **(f)** Boxplot of α values plotted against epochs. (paired t-test, p<0.05). **(g)** Line fit (dashed line) with exponent λ_{fit} to the plot of mean avalanche size $< S >$ conditioned on a specific duration T and duration T. **(h)** Boxplot of mean $\lambda_{predict}$ and λ_{fit} values for all animals plotted against epochs. **(i)** Violin plots of distance to criticality coefficient (DCC) plotted against epochs. **(j)** Mean boxplots of DCC for all epochs plotted against animals. **(k)** Mean branching parameter (σ) for all animals plotted against epochs. **(l)** Mean α values plotted against mean σ values for all epochs. Grey dashed lines represent the mean for all epochs. **(m)** Mean σ values for all epochs plotted against animals. **(n)** Box plot of mean Wasserstein distance between all ten animals.

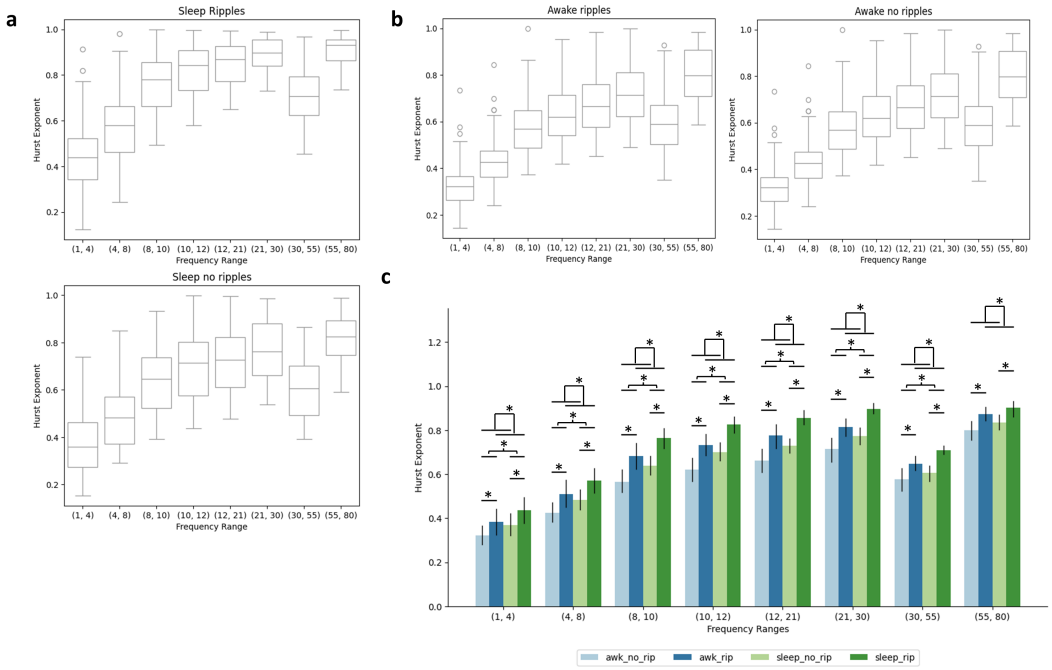

Figure 2. Time series metrics for avalanche criticality.

Mean hurst exponent for all animals in epoch **(a)** sleep ripples and sleep no ripples **(b)** awake ripples and awake no ripples in different frequency bands. **(c)** Mean hurst exponent for all animals in four epochs across frequency bands. (paired t-test, $p<0.05$).